CHEMISTRY OF MATERIALS

Article

Low-Temperature-Processible, Transparent, and Air-Operable n-Channel Fluorinated Phenylethylated Naphthalenetetracarboxylic Diimide Semiconductors Applied to Flexible Transistors

Byung Jun Jung, Jia Sun, Taegweon Lee, Amy Sarjeant, and Howard E. Katz

Chem. Mater., **Article ASAP**

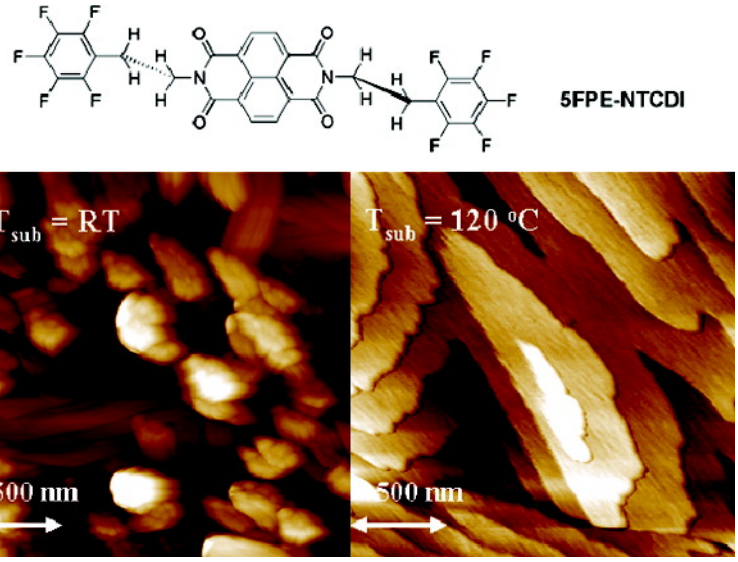

More About This Article

Additional resources and features associated with this article are available within the HTML version:

- Supporting Information
- Access to high resolution figures
- Links to articles and content related to this article
- Copyright permission to reproduce figures and/or text from this article

View the Full Text HTML

Chemistry of Materials is published by the American Chemical Society. 1155 Sixteenth Street N.W., Washington, DC 20036

Low-Temperature-Processible, Transparent, and Air-Operable n-Channel Fluorinated Phenylethylated Naphthalenetetracarboxylic Diimide Semiconductors Applied to Flexible Transistors

Byung Jun Jung,[†] Jia Sun,[†] Taegweon Lee,[†] Amy Sarjeant,[‡] and Howard E. Katz[†,‡,*]

Departments of Materials Science and Engineering and of Chemistry, Johns Hopkins University, 3400 North Charles Street, Baltimore, Maryland 21218

Received August 22, 2008. Revised Manuscript Received November 2, 2008

New *N*,*N*′-disubstituted-1,4,5,8-naphthalene tetracarboxylic acid diimides (NTCDI) with fluorinated phenylethyl groups were synthesized. In particular, *N*,*N*′-bis(2-(pentafluorophenyl)ethyl)-1,4,5,8-naphthalene tetracarboxylic acid diimide (5FPE-NTCDI) showed high electron mobility, more than 0.1 $cm^2/(V\ s)$ in air, even though the film was deposited at room temperature. The correlation of the crystallinity, morphology, and mobility with the substrate temperature during deposition (T_{sub}) was studied using X-ray diffraction (XRD) and atomic force microscopy (AFM). The films of 5FPE-NTCDI exhibited a "thin film phase", mixed phase, and crystal bulk phase as T_{sub} was increased. The mixed phase on an octadecyltrimethoxysilane (OTS)-treated substrate also has high electron mobility due to well connected long fiber-shaped grains. The high mobility at low T_{sub} has enabled fabrication of flexible transistors on the clear plastic substrate poly(ethylene terephthalate) (PET). The highest mobility for a flexible, transparent transistor was 0.23 $cm^2/(V\ s)$, obtained with low hysteresis.

Introduction

Recently, organic thin-film transistors (OTFTs) have been investigated extensively for application in technologies such as display backplanes,[1] radio frequency identification (RFID) tags,[2] and chemical sensing.[3] The mobility of some p-channel materials[4] already exceeds that of hydrogenated amorphous silicon (*a*-Si:H) even though the stability is inferior to that of *a*-Si:H.[5] However, OTFTs with sufficient lifetime can be adapted to new applications with their advantages such as lightweight and flexibility.[6] Most OTFTs have been fabricated on SiO_2/Si substrates for measurement of carrier mobility. High substrate temperature (T_{sub}) is usually required to achieve the high mobility.[7] Alternatively, high annealing temperature is needed.[8] High mobility at low T_{sub} is desirable for low-cost device fabrication, and is important for flexible electronics using plastic films. The glass temperature of common clear plastic substrates such as poly(ethylene terephthalate) (PET) and poly(ethylene naphthalate) (PEN) are 75−80 and 120 °C, respectively.[9] There have been a few reports of high mobility at lower T_{sub} and most concerned p-channel materials.[10]

Air operability is another desirable attribute of OTFTs. OTFTs with air-operable n-channels are useful for complementary circuits[11] with combined n-channel and p-channel devices providing lower power consumption than unipolar field effect transistor (FET) circuits.[1a] Following the report of naphthalenetetracarboxylic diimides (NTCDIs) with fluorinated side chains as air-stable n-channel materials,[12] several other air-stable n-channel materials[13] have been developed and some showed high mobility of up to 0.64 $cm^2/(V\ s)$ in air.[13a] However, all of them required high T_{sub} to

* Corresponding author.
† Department of Materials Science and Engineering, Johns Hopkins University.
‡ Department of Chemistry, Johns Hopkins University.

(1) (a) Gelinck, G. H.; Huitema, H. E. A.; Van Veenendaal, E.; Cantatore, E.; Schrijnemakers, L.; Van der Putten, J.; Geuns, T. C. T.; Beenhakkers, M.; Giesbers, J. B.; Huisman, B. H.; Meijer, E. J.; Benito, E. M.; Touwslager, F. J.; Marsman, A. W.; van Rens, B. J. E.; De Leeuw, D. M. *Nat. Mater.* **2004**, *3*, 106. (b) Zhou, L.; Wanga, A.; Wu, S.-C.; Sun, J.; Park, S.; Jackson, T. N. *Appl. Phys. Lett.* **2006**, *88*, 083502.
(2) Cantatore, E.; Geuns, T. C. T.; Gelinck, G. H.; van Veenendaal, E.; Gruijthuijsen, A. F. A.; Schrijnemakers, L.; Drews, S.; De Leeuw, D. M. *IEEE J. Solid-State Circ.* **2007**, *42*, 84.
(3) (a) See, K. C.; Becknell, A.; Miragliotta, J.; Katz, H. E. *Adv. Mater.* **2007**, *19*, 3322. (b) Huang, J.; Miragliotta, J.; Becknell, A.; Katz, H. E. *J. Am. Chem. Soc.* **2007**, *129*, 9366. (c) Huang, J.; Sun, J.; Katz, H. E. *Adv. Mater.* **2008**, *20*, 2567.
(4) (a) Payne, M. M.; Parkin, S. R.; Anthony, J. E.; Kuo, C.-C.; Jackson, T. N. *J. Am. Chem. Soc.* **2005**, *127*, 4986. (b) Takimiya, K.; Ebata, H.; Sakamoto, K.; Izawa, T.; Otsubo, T.; Kunugi, Y. *J. Am. Chem. Soc.* **2006**, *128*, 12604. (c) Yamamoto, T.; Takimiya, K. *J. Am. Chem. Soc.* **2007**, *129*, 2224. (d) Ebata, H.; Izawa, T.; Miyazaki, E.; Takimiya, K.; Ikeda, M.; Kuwabara, H.; Yui, T. *J. Am. Chem. Soc.* **2007**, *129*, 15732.
(5) Hekmatshoar, B.; Cherenack, K. H.; Kattamis, A. Z.; Long, K.; Wagner, S.; Sturm, J. C. *Appl. Phys. Lett.* **2008**, *93*, 032103.
(6) Forrest, S. R. *Nature* **2004**, *428*, 911.
(7) Murphy, A. R.; Fréchet, J. M. J. *Chem. Rev.* **2007**, *107*, 1066.
(8) Tatemichi, S.; Ichikawa, M.; Koyama, T.; Taniguchi, Y. *Appl. Phys. Lett.* **2006**, *89*, 112108.
(9) (a) Jabarin, S. A. *Polym. Eng. Sci.* **1992**, *32*, 1341. (b) Saiter, A.; Hess, M.; Saiter, J. M.; Grenet, J. *Macromol. Symp.* **2001**, *174*, 165.
(10) (a) Sun, Y.; Ma, Y.; Liu, Y.; Lin, Y.; Wang, Z.; Wang, Y.; Di, C.; Xiao, K.; Chen, X.; Qiu, W.; Zhang, W.; Yu, G.; Hu, W.; Zhu, D. *Adv. Funct. Mater* **2006**, *16*, 426. (b) Du, C.; Guo, Y.; Liu, Y.; Qiu, W.; Zhang, H.; Gao, X.; Liu, Y.; Qi, T.; Lu, K.; Yu, G. *Chem. Mater.* **2008**, *20*, 4188. (c) Seo, H.-S.; Zhang, Y.; Jang, Y.-S.; Choi, J.-H. *Appl. Phys. Lett.* **2008**, *92*, 223310. (d) Tang, M. L.; Reichardt, A. D.; Okamoto, T.; Miyaki, N.; Bao, Z. *Adv. Funct. Mater.* **2008**, *18*, 1579.
(11) Crone, B.; Dodabalapur, A.; Lin, Y. Y.; Filas, R. W.; Bao, Z.; LaDuca, A.; Sarpeshkar, R.; Katz, H. E.; Li, W. *Nature* **2000**, *403*, 521.
(12) (a) Katz, H. E.; Lovinger, A. J.; Johnson, J.; Kloc, C.; Siegrist, T.; Li, W.; Lin, Y. Y.; Dodabalapur, A. *Nature* **2000**, *404*, 478. (b) Katz, H. E.; Johnson, J.; Lovinger, A. J.; Li, W. *J. Am. Chem. Soc.* **2000**, *122*, 7787.

10.1021/cm802281k CCC: $40.75

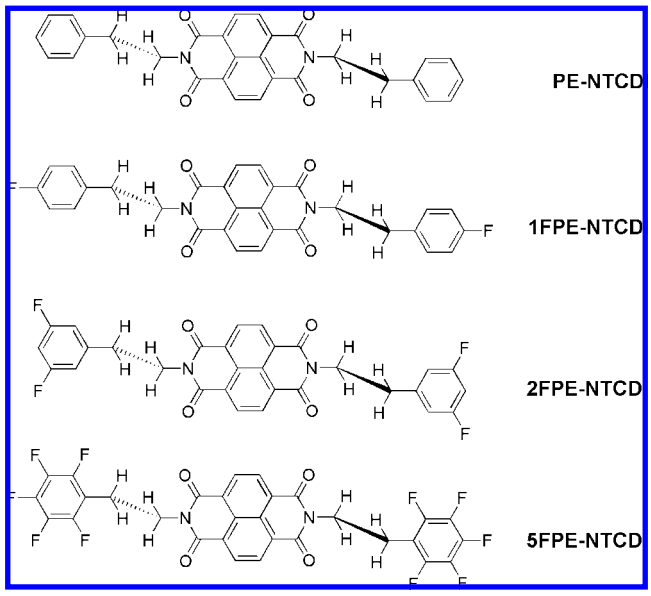

Figure 1. Chemical structures of the new NTCDI derivatives.

achieve maximum mobility. In this paper, we report new NTCDIs with fluorinated phenylethyl groups, in particular *N*,*N*′-bis(2-(pentafluorophenyl)ethyl)-1,4,5,8-naphthalene tetracarboxylic acid diimide (5FPE-NTCDI), as air-operable n-channel materials, with a degree of air stability (Figure 1). X-ray diffraction (XRD) and atomic force microscopy (AFM) of the thin films reveal highly crystalline morphologies, in contrast to the relatively amorphous NTCDI with pentafluorophenyl groups.[12b] To the best of our knowledge, this paper is the first report of electron mobility over 0.1 $cm^2/(V\ s)$ for an air-operable n-channel OTFT deposited at low T_{sub} at or near ambient. Moreover, we demonstrate flexible and transparent OTFTs with mobility of up to 0.23 $cm^2/(V\ s)$ on clear, plastic PET film, with low hysteresis. Results for 5FPE-NTCDI are compared with other phenethyl NTCDI analogs, and the effect of the dielectric surface on OTFT hysteresis is also considered.

Results and Discussion

Many NTCDI and PTCDI (perylenetetracarboxylic diimide) derivatives have been synthesized and reported as n-channel semiconductors, mostly using commercially available amines.[3] Some aryl acetonitrile compounds are commercially available and their useful reduction of nitriles to amines was reported by Nystrom.[14a] We synthesized new NTCDI derivatives by reacting naphthalene tetracarboxylic dianhydride (NTCDA) with the fluorinated phenyl ethyl amines obtained from the corresponding nitriles (Scheme 1). Reasonable yields (63−78%) were obtained, even after repeated sublimation. Single crystals of 1FPE-NTCDI, 2FPE-NTCDI and 5FPE-NTCDI were obtained during sublimation, and the crystal structures were determined by X-ray structure analysis (Figures 1S−3S in the Supporting Information). However, the size of the crystals of 5FPE-NTCDI was not large enough for exact analysis, so the structure determination of 5FPE-NTCDI was incomplete. As expected, the molecular structures of the compounds are similar. The two phenyl rings of both sides of the molecules are parallel to the naphthalene ring of the center because the molecules are in stable anti conformations. Meanwhile, the packing structures are quite different. The molecules of 1FPE-NTCDI are arranged in a zigzag fashion along the *c* axis. The $\pi-\pi$ planes are stacked along the *a* axis with a smallest intermolecular C−C distance of 3.249 Å. Notably, the phenyl rings of 2FPE-NTCDI are located near neighboring center rings along the *b* axis. Although a closest C−C distance in the stack of 2FPE-NTCDI is also as short as 3.31 Å, the naphthalene-imide ring systems do not overlap each other along a closest $\pi-\pi$ distance. Moreover, the π-stacking distance (*a* axis = 6.622 Å) of 2FPE-NTCDI is longer than that of 1FPE-NTCDI (*b* axis= 4.895 Å) because of the interruption of the phenyl rings along the *b* axis. This packing structure of 2FPE-NTCDI does not appear effective for carrier transport.

OTFT devices on SiO_2/Si were fabricated in the top contact configuration. The devices made from PE-NTCDI (nonfluorinated) and 2FPE-NTCDI showed little or no n-channel transistor activity in air. However, the devices made from 1FPE-NTCDI showed typical n-channel transistor characteristics in air even though only one fluorine was attached to each phenyl ring (Figure 2a). The lack of n-channel behavior of 2FPE-NTCDI may be due to unfavorable crystal packing. All devices made from 5FPE-NTCDI showed typical n-channel transistor characteristics in air with high on/off ratio. Compared to 1FPE-NTCDI OTFTs, 5FPE-NTCDI OTFTs showed much less hysteresis during off−on and off−on sweeps (panels a and b in Figure 2). Recently, Gu et al.[15a] reported that the water vapor was the cause of hysteresis-causing traps rather than oxygen in the case of pentacene OTFTs in air. Also, Umeda et al.[15b] reported that pentacene OTFTs with fluoropolymer as gate insulator exhibited negligible current hysteresis in ambient air. Thus, introducing fluorines to the molecule (or the gate dielectric) can reduce the hysteresis. Also, once again, a heavily fluorinated side chain is associated with high electron mobility in air.

Device data for each surface treatment are shown in Table 1. (Figure 4S in the Supporting Information shows the field-effect mobility of 5FPE-NTCDI devices as a function of substrate temperature.) OTS devices show higher mobility than HMDS devices, consistent with several previous OTFT

(13) (a) Jones, B. A.; Ahrens, M. J.; Yoon, M.-H.; Facchetti, A.; Marks, T. J.; Wasielewski, M. R. *Angew. Chem., Int. Ed.* **2004**, *43*, 6363. (b) Chen, H. Z.; Ling, M. M.; Mo, X.; Shi, M. M.; Wang, M.; Bao, Z. *Chem. Mater.* **2007**, *19*, 816. (c) Jones, B. A.; Facchetti, A.; Marks, T. J.; Wasielewski, M. R. *Chem. Mater.* **2007**, *19*, 2703. (d) Ling, M.-M.; Erk, P.; Gomez, M.; Koenemann, M.; Locklin, J.; Bao, Z. *Adv. Mater.* **2007**, *19*, 1123. (e) Schmidt, R.; Ling, M. M.; Oh, J. H.; Winkler, M.; Könemann, M.; Bao, Z.; Würthner, F. *Adv. Mater.* **2007**, *19*, 3692. (f) Oh, J. H.; Liu, S.; Bao, Z.; Schmidt, R.; Würthner, F. *Appl. Phys. Lett.* **2007**, *91*, 212107. (g) Jones, B. A.; Facchetti, A.; Wasielewski, M. R.; Marks, T. J. *Adv. Funct. Mater.* **2008**, *18*, 1329. (h) See, K. C.; Landis, C.; Sarjeant, A.; Katz, H. E. *Chem. Mater.* **2008**, *20*, 3609. (i) Weitz, R. T.; Amsharov, K.; Zschieschang, U.; Villas, E. B.; Goswami, D. K.; Burghard, M.; Dosch, H.; Jansen, M.; Kern, K.; Klauk, H. *J. Am. Chem. Soc.* **2008**, *130*, 4637. (j) Song, D.; Wang, H.; Zhu, F.; Yang, J.; Tian, H.; Geng, Y.; Yan, D. *Adv. Mater.* **2008**, *20*, 2142.
(14) (a) Nystrom, R. F. *J. Am. Chem. Soc.* **1955**, *77*, 2544. (b) Filler, R.; Chen, W.; Woods, S. M. *J. Fluorine Chem.* **1995**, *73*, 95.
(15) (a) Gu, G; Kane, M. G. *Appl. Phys. Lett.* **2008**, *92*, 053305. (b) Umeda, T.; Kumaki, D.; Tokito, S. *Org. Electron.* **2008**, *9*, 545.

Scheme 1. Synthesis of NTCDI Derivatives[a]

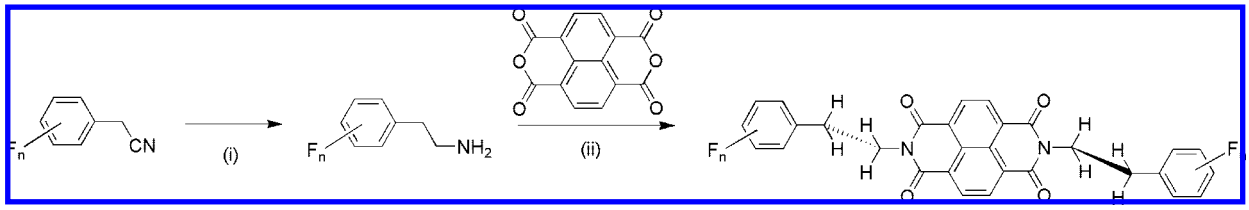

[a] (i) $LiAlH_4$-$AlCl_3$ (1:1), ether, RT, 1 h; (ii) $Zn(OAc)_2$, quinoline, 190 °C, overnight.

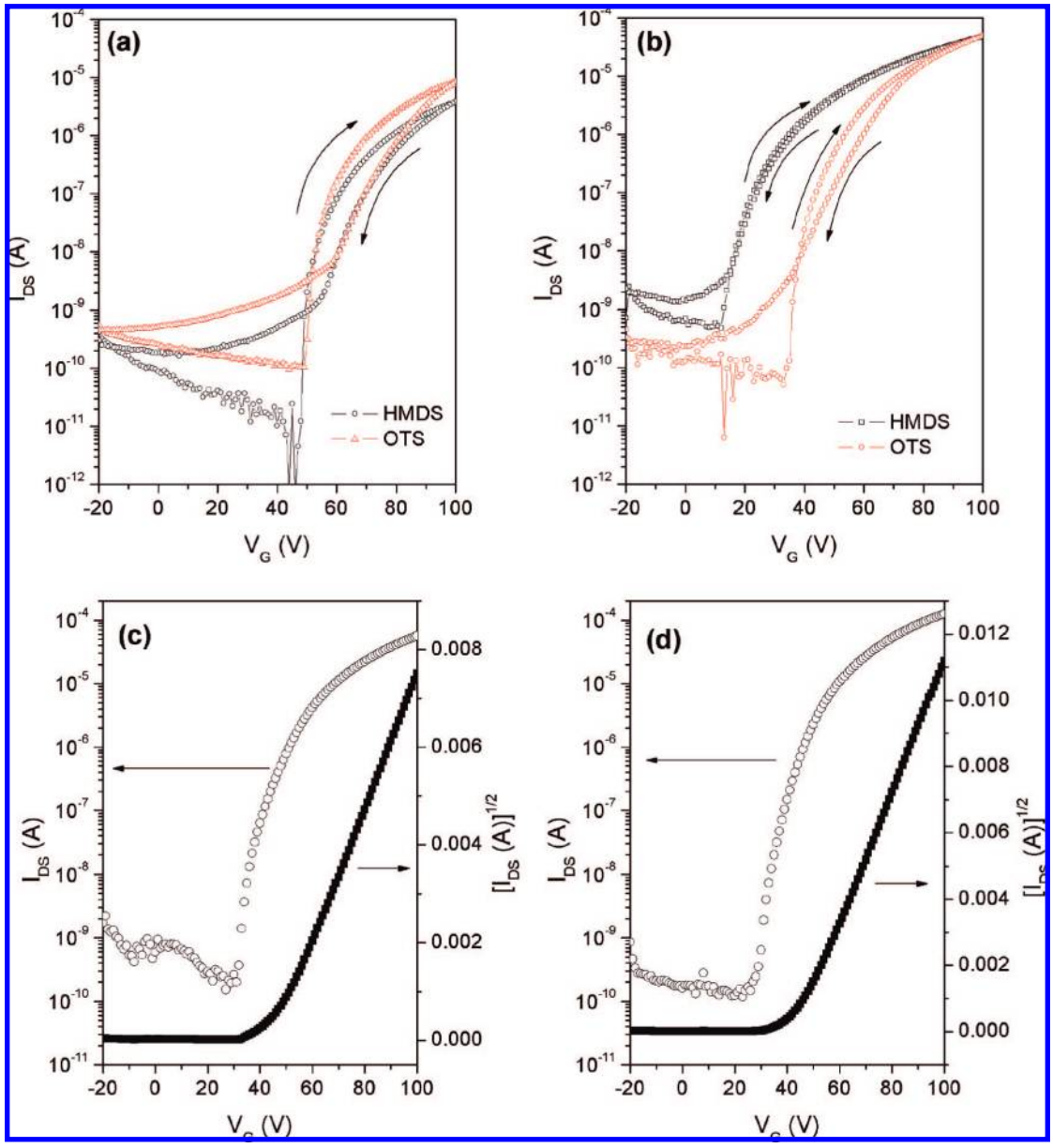

Figure 2. Typical transfer characteristics of (a) 1FPE-NTCDI and (b) 5FPE-NTCDI OTFTs deposited at RT and of 5FPE-NTCDI OTFT (c) deposited at RT (μ = 0.14 cm^2/(V s)) and (d) at 40 °C (μ = 0.31 cm^2/(V s)) on the OTS-treated substrate.

reports.[4b,c,10c,13d] Some groups have studied the relationship between the mobility and surface treatment using synchrotron two-dimensional grazing-incidence X-ray diffraction (2D GIXD),[16] and explained that the most effective surface treatments for high mobility produce well-ordered crystallites. Some of our 5FPE-NTCDI devices show very high on/off ratio greater than 1×10^7. Also, some freshly prepared devices have a very low subthreshold swing, <1 V/decade, even though a thick dielectric layer (300 nm of SiO_2) was used (see Figure 5S in the Supporting Information). High on/off ratio and low subthreshold swing point to this compound as an excellent candidate for n-channel organic transistors. Interestingly, the mobility for OTS devices was greater than 0.1 cm^2/(V s), even though their substrate

Table 1. Summary of the Characteristics of OTFT in Air Using Various Substrate Deposition Temperatures

OSC	surface treatment	T_{sub} (°C)	μ (cm^2/(v s))	max μ (cm^2/(v s))	I_{on}/I_{off}	V_t (V)	SS (V/decade)	no. devices tested
1FPE- NTDCI	HMDS	RT	0.017 ± 0.003	0.020	$10^4 - 10^6$	53−39	1.6−3.1	3
		80	0.036 ± 0.007	0.042	$10^3 - 10^4$	41−52	4.9−6.6	3
	OTS	RT	0.043 ± 0.005	0.046	$10^4 - 10^5$	57−60	1.5−1.9	3
		80	0.060 ± 0.009	0.068	$10^5 - 10^7$	15−40	1.7−2.9	3
5FPE- NTDCI	HMDS	RT	0.064 ± 0.017	0.077	10^5	22−49	2.4−4.1	5
		40	0.052 ± 0.017	0.070	$10^4 - 10^5$	22−35	3.1−6.9	7
		60	0.091 ± 0.020	0.11	$10^5 - 10^7$	29−41	2.4−3.0	7
		80	0.15 ± 0.05	0.24	$10^4 - 10^7$	34−50	1.9−6.7	7
		100	0.12 ± 0.02	0.14	$10^4 - 10^7$	17−45	1.2−3.5	6
		120	0.19 ± 0.07	0.27	$10^4 - 10^7$	10−42	1.6−4.6	7
	OTS	RT	0.12 ± 0.03	0.14	$10^4 - 10^7$	46−51	1.7−4.7	6
		40	0.19 ± 0.07	0.31	$10^4 - 10^7$	31−52	1.7−5.4	12
		60	0.17 ± 0.05	0.20	$10^5 - 10^7$	10−69	1.4−2.2	7
		80	0.20 ± 0.02	0.22	$10^6 - 10^7$	9−56	1.5−2.3	5
		100	0.16 ± 0.01	0.16	$10^5 - 10^7$	54−61	1.5−3.9	4
		120	0.22 ± 0.02	0.26	$10^4 - 10^6$	15−55	1.7−4.7	8
	OTS[a]	RT	0.11 ± 0.01	0.13	10^5	10−11	1.4−1.5	8
		40	0.17 ± 0.02	0.22	$10^5 - 10^6$	8−14	1.0−1.5	16
		80	0.13 ± 0.02	0.16	$10^6 - 10^7$	5−8	0.6−1.1	6
		120	0.17 ± 0.02	0.20	$10^6 - 10^7$	4−7	0.7−1.2	7

[a] From the scane of the transfer curve between −10 and 50 V of V_g without having scanned the output curves up tot 100 V of V_g, to minimize the possible effects of bias stress.

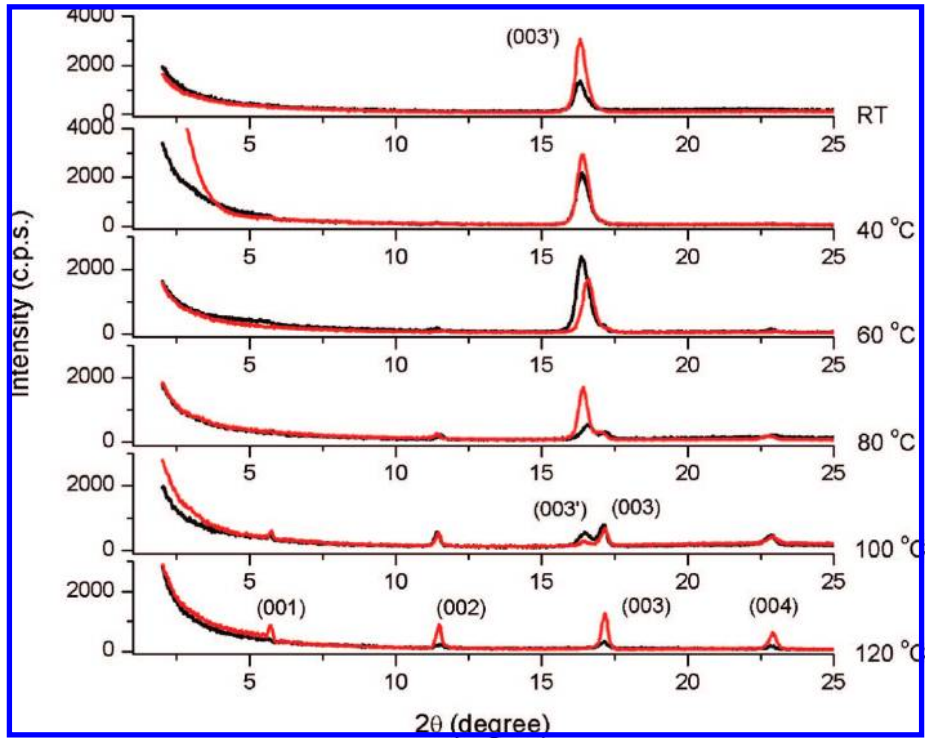

Figure 3. X-ray diffraction patterns for 5FPE-NTCDI deposited films at the indicated T_{sub} values on HMDS-treated substrate (black lines) and OTS-treated substrate (red lines).

temperature during deposition was room temperature (25 °C). Moreover, the highest mobility of 0.31 cm^2/(V s) was obtained at a deposition temperature of 40 °C (Figure 2d) in contrast to other NTCDI and PTCDI derivatives[13] that showed the highest mobility requiring at least 75 °C for T_{sub}. Average mobilities for this type of device were fairly insensitive to temperature. Thus, 5FPE-NTCDI offers an opportunity for fabrication of transparent and flexible organic transistor backplanes and low-cost devices without increasing substrate temperature.

The average mobility at T_{sub} of 40 °C was comparable to that from T_{sub} of 120 °C. This is unusual compared to the observation in many organic transistor semiconductors that mobility rises with increasing substrate temperature during thin film deposition, due to increased crystallinity and larger grain sizes.[13d−g] However, 5FPE-NTCDI films deposited at RT and 40 °C showed good crystallinity with strong peaks at 16.3° in $\theta-2\theta$ X-ray diffraction patterns (Figure 3). A new peak at 17.1° accompanied by higher-order peaks appeared in addition to the one at 16.3° starting with 60 °C, and finally the peaks that are associated with low T_{sub} disappeared at T_{sub} of 120 °C. The first-order peak for T_{sub} of 120 °C was 5.7°, corresponding to a lattice spacing of

(16) (a) Kline, R. J.; Mcgehee, M. D.; Toney, M. F. *Nat. Mater.* **2006**, *5*, 222. (b) Kim, D. H.; Lee, H. S.; Yang, H.; Yang, L.; Cho, K. *Adv. Funct. Mater.* **2008**, *18*, 1363.

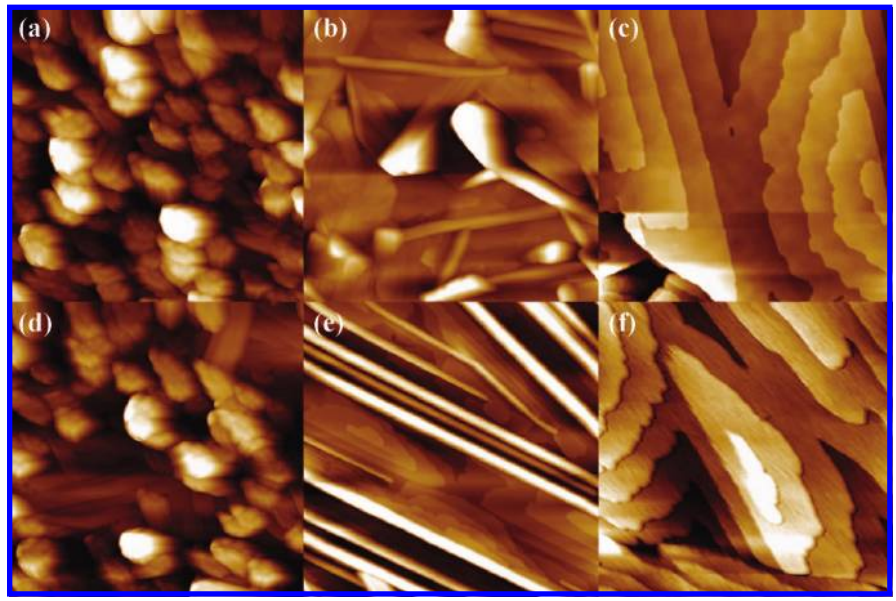

Figure 4. $2 \times 2\ \mu m^2$ AFM topography images of 5FPE-NTCDI deposited films on the two different surface-treated SiO_2/Si substrates at different T_{sub}: (a) HMDS, RT; (b) HMDS, 80 °C; (c) HMDS 120 °C; (d) OTS, RT; (e) OTS, 80 °C; (f) OTS, 120 °C.

15.5 Å. Single-crystalline 5FPE-NTCDI exhibits a *c*-axis of 31.4 Å, which consists of two molecules, and β of 97.9° (see Figure S4 in the Supporting Information). Therefore, in such a structure, the 001 plane spacing d_{001} is 15.5 Å (= 1/2 × *c*-axis × sin β). This agrees with the first order peak at 120 °C, so the four reflections at 120 °C can be indexed as (00*l*) reflections from the crystal bulk phase of the material. The strong peak of 16.3° in the low-temperature phase is a (003′) reflection corresponding to a lattice spacing of 16.3 Å. This can also be considered a "thin film phase", kinetically favored.[17] It is difficult to say that the crystal bulk phase is superior to the thin film phase for electron transport because they are both crystalline and highly ordered.[17c] This may explain why the mobility of devices deposited at 40 °C is comparable to that of 120 °C devices.

Between 60 and 100 °C, the films are of mixed phase. In previous experiments, the mixed-phase films had transport properties inferior to films consisting solely of one phase.[17b] In pentacene, the mobility of a highly mixed phase, in which the ratio was nearly 1:1, was remarkably low,[17a] but the mobility of mixed phases where the minor component was only about 10% mixed devices was mostly maintained. The mobility of several PTCDI compounds can be an order magnitude lower for low T_{sub} than for $T_{sub} > 70$ °C.[13b,f,g,i] However, for our OTS devices, the mobility from 100 °C deposition was somewhat lower than that of 80 °C devices, and there was little change of mobility at lower T_{sub}. This suggests that the two phases of 5FPE-NTCDI have similar molecular alignments and good overlap at the grain boundary.

Another important factor related to the carrier mobility is the grain size. Generally, larger grain sizes provide higher mobility. Figure 4 shows AFM images of 5FPE-NTCDI. As generally observed for films of organic semiconductor materials, the grain size of 5FPE-NTCDI films becomes larger as the T_{sub} increases. Our new NTCDI films at T_{sub} = RT already show over several hundred nm of grain size, which is comparable to that of other PTCDI films deposited at 90 °C.[13d,f] For further comparison, grain size is about 0.5−0.8 μm in pentacene[17c,18] Moreover, some 5FPE-NTCDI grains on OTS surfaces grow laterally up to 1 μm. This explains how our device on OTS showed high mobility from RT to high T_{sub}. The rod shaped grains are formed at low T_{sub} and the plate shaped grains are formed at high T_{sub}. The former corresponds to the thin film phase and the latter to the crystal bulk phase. As expected from XRD results, the films of T_{sub} = 80 °C show both rods and terraced plates. Obvious terraces are observed in films deposited at 120 °C and the height is around 15 Å, well-matched to XRD results (see Figure 6S in the Supporting Information). The size is 2−3 μm (see Figure 7S in the Supporting Information). The thin-film morphology at 120 °C shows no apparent difference depending on the surface treatment, but in the mixed-phase region, there is a significant difference. In the films on HMDS, the rod type grains become larger as the T_{sub} increases, and then become mixed with plate type grains. Interestingly, in the films on OTS, the rod type grain appears as a long fiber type grain of several μm. This explains the consistent mobility of the OTS devices at various T_{sub} even though the morphology under some conditions is mixed phase.

We attempted thermal annealing of the RT and 120 °C devices at 200 °C for 1 h in the vacuum oven. The RT device lost its ability to function as a transistor. The performance of the 120 °C device was slightly diminished.

To test device stability, we stored a high-performing OTS device with mobility of 0.31 $cm^2/(V\ s)$ in air and under office light for 1 month (see Figure 9S and Table 1S in the Supporting Information). The device still showed n-channel OTFT characteristics in air. The mobility, threshold voltage and on/off ratio

(17) (a) Dimitrakopoulos, C. D.; Brown, A. R.; Pomp, A. *J. Appl. Phys.* **1996**, *80*, 2501. (b) Gundlach, D. J.; Jackson, T. N.; Schlom, D. G.; Nelson, S. F. *Appl. Phys. Lett.* **1999**, *77*, 3302. (c) Knipp, D.; Street, R. A.; Völkel, A.; Ho, J. *J. Appl. Phys.* **2003**, *93*, 347. (d) Chesterfield, R. J.; McKeen, J. C.; Newman, C. R.; Ewbank, P. C.; Filho, D. A.; da, S.; Brédas, J.-L.; Miller, L. L.; Mann, K. R.; Frisbie, C. D. *J. Phys. Chem. B* **2004**, *108*, 19281. (e) Petit, M.; Hayakawa, R.; Wakayama, Y.; Chikyow, T. *J. Phys. Chem. C* **2007**, *111*, 12747.

(18) Kim, C.; Facchetti, A.; Marks, T. J. *Science* **2007**, *318*, 76.

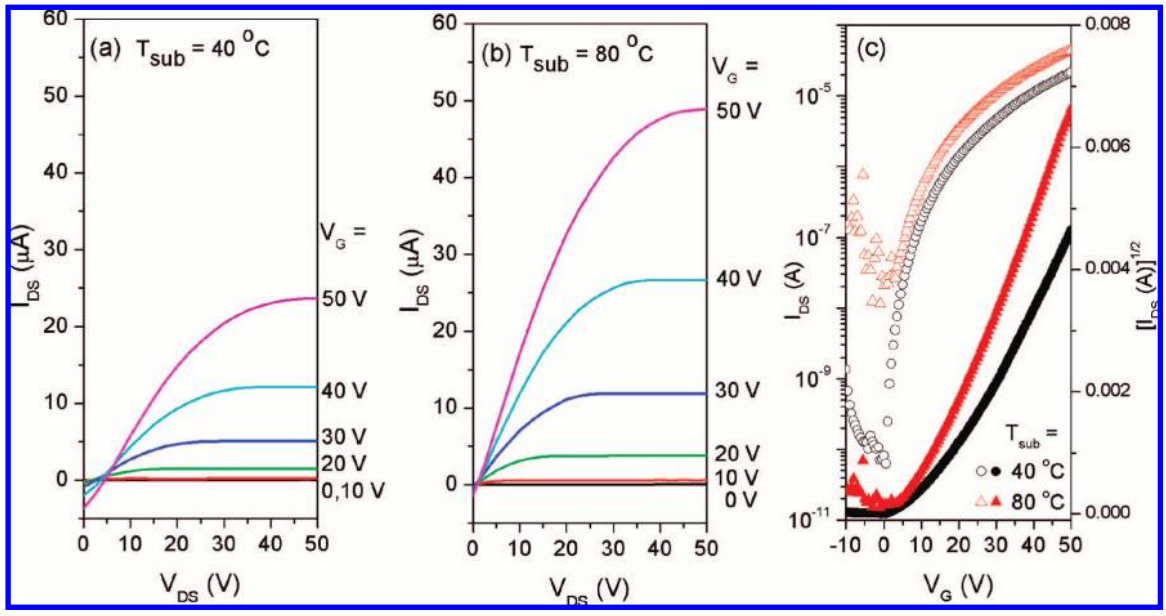

Figure 5. Typical output curves of the flexible and transparent 5FPE-NTCDI OTFTs deposited at (a) 40 and (b) 80 °C on an ITO/PET film with a PMMA polymer dielectric layer and (c) transfer curves of them. Open shapes, log scale; closed shapes, square root of current. I_{DS} does not contain contributions from I_G. The magnitude of I_G is indicated in Figure 7 (bending data).

were changed from 0.31 cm^2/(V s), 45 V, 1.1×10^6 to 0.18 cm^2/(V s), 74 V, 3.0×10^4, respectively. Recovery of the threshold voltage and on/off ratio was possible by returning the device to a vacuum. After one day under a vacuum, the device showed a well-formed transfer curve with low subthreshold swing of 1.1 V/decade in a vacuum, a performance that was stable in a vacuum. The on/off ratio in a vacuum was higher and threshold voltage was shifted more negative than that of the initial device in air. This could correspond to the removal of oxygen in a vacuum, which was absorbed in the organic layer or at the interface between semiconductor and dielectric layer and acted as a deep trap.[19] The threshold voltage of the device after re-exposure to air moved close to its initial value in air. Similar threshold voltage drifts occurred when the air exposure was in a 100 °C oven, suggesting that oxygen was a more important factor than water in causing these drifts. Threshold voltage magnitudes and shifts were smaller for 5PFE-NTCDI-on-PMMA devices: 8 V on a fresh device, drifting to 22 V over a few days. Drifts of similar magnitudes over timescales of days have been reported for other n-channel organic semiconductors[13f,j] that were also deemed "air stable".

Encapsulation of the 5FPE-NTCDI-on-OTS device with an overcoating of CYTOP fluorinated polymer helped stabilize the threshold voltage and mobility to air exposure, though the encapsulation itself caused a 3-fold drop in the mobility. The data are plotted in Figure 6. Although both parameters drifted considerably for the case of the unencapsulated device, the CYTOP encapsulation significantly retarded the drift, to negligible amounts during the 10 h time scale of the experiment. This indicates a possible route to avoiding unacceptable changes in device parameters during use, at least over moderate time periods. A vapor-deposited film of p-quinquephenyl also prevented threshold voltage drift, though mobility did decrease from 0.11 to 0.055 cm^2/(V s) over 5 days in air, before stabilizing. Additional data related to device stability are presented in the Supporting Information.

The transparent and flexible n-channel OTFTs were fabricated with 5FPE-NTCDI on clear plastic PET film coated with ITO. There are several previous reports of cross-linked poly(4-vinylphenol) (PVP) as dielectric layers.[20] However, high process temperature (175−200 °C) is needed to cross-link PVP. Recently, a composite of inorganic nanoparticle and polymer was reported but this also required high baking temperatures.[21] We selected poly(methylmethacrylate) (PMMA)[20b] and processed it at 70 °C. NTCDI films which we deposited on PMMA/ITO/PET were highly transparent. Thin gold stripes of 20 nm were evaporated as source and drain electrodes. The gate-dielectric-semiconductor trilayers are transparent enough to read text through them (see Figure 10S in the Supporting Information). The typical flexible n-channel OTFTs of T_{sub} = 40 and 80 °C exhibit 0.14 and 0.23 cm^2/(V s) mobility, 5.6×10^5 and 3.9×10^3 of on/off ratio, 16 and 4 V of threshold voltage, and 1.2 and 2.5 V/decade of subthreshold swing, respectively (Figure 5). To the best of our knowledge, 0.23 cm^2/(V s) is highest electron mobility among flexible OTFTs in air. The characteristics of the devices on PET are summarized in Table 2. When thin painted PEDOT-PSS source-drain electrodes are used, the entire device is essentially transparent (see Figure 10Sd in the Supporting Information). This device shows n-channel OTFT characteristics with somewhat less mobility than the device in which Au electrodes are used.

(19) Chesterfield, R. J.; McKeen, J. C.; Newman, C. R.; Frisbie, C. D.; Ewbank, P. C.; Mann, K. R.; Miller, L. L. *J. Appl. Phys.* **2004**, *95*, 6396.

(20) (a) Klauk, H.; Halik, M.; Zschieschang, U.; Schmid, G.; Radlik, W.; Weber, W. *J. Appl. Phys.* **2002**, *92*, 5259. (b) Zhou, J.; Zhang, F.; Lan, L.; Wen, S.; Peng, J. *Appl. Phys. Lett.* **2007**, *91*, 253507. (c) Sethuraman, K.; Ochiai, S.; Kojima, K.; Mizutani, T. *Appl. Phys. Lett.* **2008**, *92*, 183302.

(21) Kim, P.; Zhang, X.-H.; Domercq, B.; Jones, S. C.; Hotchkiss, P. J.; Marder, S. R.; Kippelen, B.; Perry, J. W. *Appl. Phys. Lett.* **2008**, *93*, 013302.

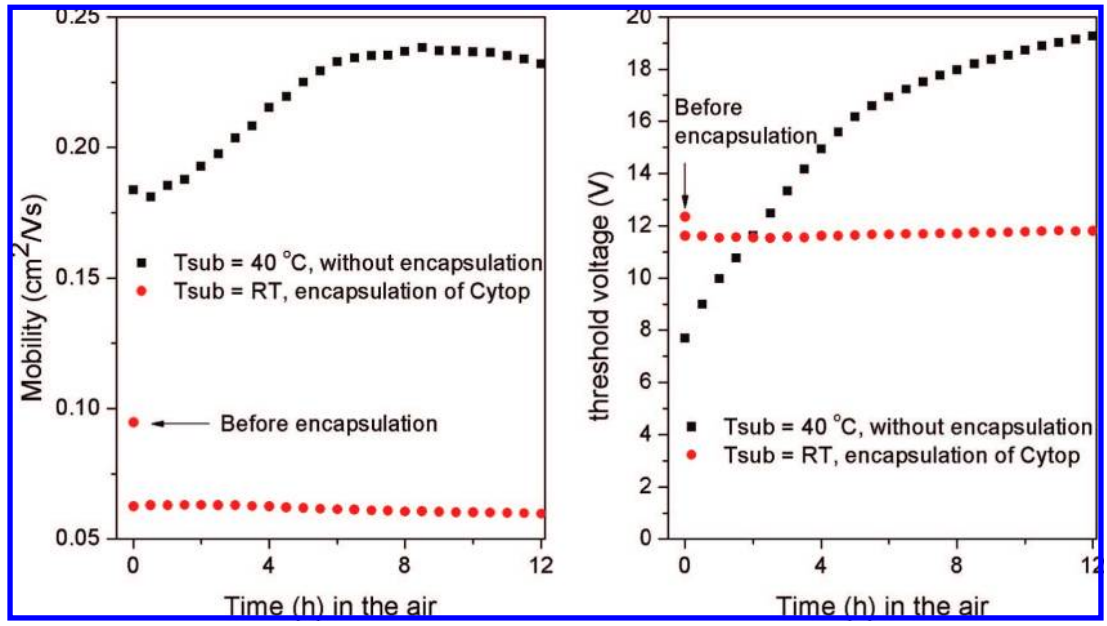

Figure 6. Mobility and threshold voltage as a function of air exposure time for a 5FPE-NTCDI-on-OTS device.

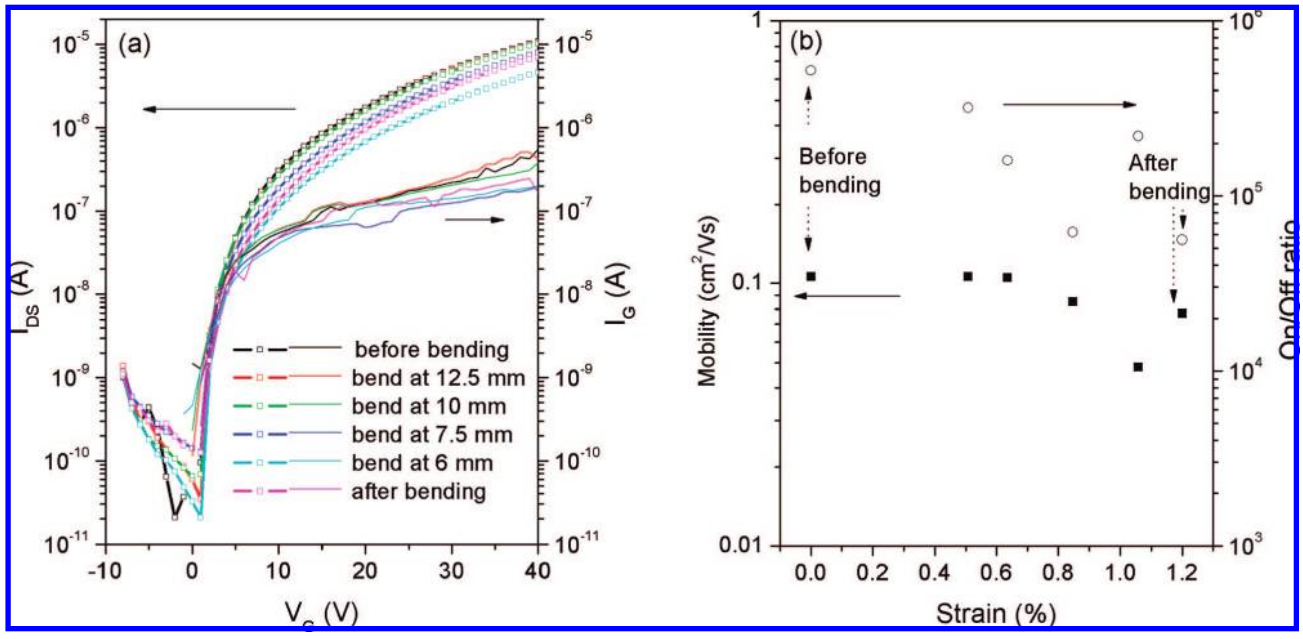

Figure 7. (a) Transfer curves and gate leakage currents at different bending radii. (b) Mobility as a function of tensile strain, for experiments listed in Table 3.

Table 2. Summary of the Characteristics of Flexible and Transparent 5FPE-NTCDI OTFT in Air at Various Substrate Deposition Temperatures

T_{sub} (°C)	μ (cm^2/(v s))	max μ (cm^2/(v s))	I_{on}/I_{off}	V_t (V)	SS (V/decade)
RT	0.078 ± 0.020	0.097	$10^3 - 10^5$	11−18	1.2−2.5
40	0.12 ± 0.03	0.14	10^5	16−18	1.2−1.8
60	0.15 ± 0.01	0.16	$10^2 - 10^5$	6−14	1.4−6.3
80	0.19 ± 0.04	0.23	$10^2 - 10^3$	4−14	2.7−3.6

The flexible transistor showed little change in mobility resulting from mechanical bending to a radius of 10 mm (0.64% strain) (Table 3 and Figure 7). These results are similar to the pentacene and rubrene devices reported in the literature;[22] a pentacene transistor showed a 3% change in mobility at 0.5% strain, and a rubrene transistor showed little change at 0.74% strain. When the radius was decreased to 6 mm (1.06% strain), the mobility dropped to 45% of its initial value, and subsequently recovered to 73% of its initial value on restoration to the unbent state. The on/off ratio drifted somewhat lower during these experiments, but was maintained close to 1×10^5 throughout.

We tried to deposit 5FPE-NTCDI at 100 °C but the PET film warped during heating of the substrate. In the output curve of the 40 °C device, some gate leakage was observed

Table 3. Effect of Bending (Curvature Parallel to Channel Length) on μ and V_t for Typical 5FPE-NTCDI OFET on PET

	before bending	bent at 12.5 mm radius	bent at 10 mm radius	bent at 7.5 mm radius	bent at 6 mm radius	after bendng
strain (%)	0	0.51	0.64	0.85	1.06	
μ (cm^2/(V s))	0.106	0.106	0.105	0.085	0.048	0.077
I_{on}/I_{off}	5.2×10^5	3.2×10^5	1.6×10^5	6.2×10^4	2.2×10^5	5.6×10^4
V_t (V)	8.7	9.5	9.4	10.1	10.1	10.6
SS (V/decade)	1.6	1.2	1.2	1.5	1.2	1.9
strain, $\varepsilon = d_s/2R$[22b,a]						

[a] d_s is the thickness of the substrate; PET film: 5 mil. = 0.005 in. = 0.127 mm; R is bending radius.

(Figure 5a). It is known that PMMA devices showed little hysteresis in contrast to PVP devices, but those were C_{60} n-channel OTFTs in vacuum.[20b] In that case, PMMA, which nominally has no OH groups, induced little hysteresis in the absence of water and oxygen. Our 5FPE-NTCDI devices with PMMA as gate insulator showed little hysteresis in ambient air (Figure 5c). This characteristic is attributed to the combination of a semiconductor resistant to water and oxygen and a dielectric layer without OH substituents.

Conclusion

New NTCDI compounds with fluorinated phenylethyl groups were developed as air-stable n-channel organic semiconducting materials. The electron mobility of OTS-treated OTFTs in air remained over 0.1 cm^2/(V s) at all deposition substrate temperatures. For 5FPE-NTCDI, the thin film phase obtained at low T_{sub} was sufficient for electron transport. In addition, we have successfully fabricated transparent and flexible n-channel OTFTs with electron mobility of up to 0.23 cm^2/(V s) in air. Our results suggest that n-channel organic semiconducting materials can be used for easily processed flexible OTFT circuits in air.

Experimental Section

Materials Synthesis. Phenylethylamine and 4-fluorophenylethylamine were purchased from Alfa Aesar and AK Scientific, Inc., respectively. 2,4-Difluorophenyethylamine and pentafluorophenylethylamine were synthesized as according to published procedures.[14] NTCDI derivatives were synthesized as reported[12b] previously. The naphthalenetetracarboxylic dianhydride (Aldrich) was reacted with each amine (3 mol equiv.) in quinoline with zinc acetate (0.7 mol equiv.) as the catalyst. Crude solid was then purified twice by vacuum sublimation.

***N,N′*-Di(phenylethyl)-1,4,5,8-naphthalene Tetracarboxylic Acid Diimide (PE-NTCDI).** The total yield including sublimation was 69% (light salmon color solid). Mp 284 °C. Elemental anal. Calcd for $C_{30}H_{22}N_2O_4$: C, 75.94; H, 4.67; N, 5.90. Found: C, 75.91; H, 4.60; N, 5.81.

***N,N′*-Di(4-fluorophenylethyl)-1,4,5,8-naphthalene Tetracarboxylic Acid Diimide (1FPE-NTCDI).** The total yield including sublimation was 72% (light salmon color solid). Mp 279 °C. Elemental anal. Calcd for $C_{30}H_{20}F_2N_2O_4$: C, 70.58; H, 3.95; N, 5.49. Found: C, 70.64; H, 3.84; N, 5.40.

***N,N′*-Di(3,5-difluorophenylethyl)-1,4,5,8-naphthalene Tetracarboxylic Acid Diimide (2FPE-NTCDI).** The total yield including sublimation was 63% (gray solid). Mp 287 °C. Elemental anal. Calcd for $C_{30}H_{18}F_4N_2O_4$: C, 65.94; H, 3.32; N, 5.13. Found: C, 65.97; H, 3.29; N, 5.27.

***N,N′*-Bis(pentafluorophenylethyl)-1,4,5,8-naphthalene Tetracarboxylic Acid Diimide (5FPE-NTCDI).** The total yield including sublimation was 77% (beige color solid). Mp 333 °C. Elemental anal. Calcd for $C_{30}H_{12}F_{10}N_2O_4$: C, 55.06; H, 1.85; N, 4.28. Found: C, 55.10; H, 1.79; N, 4.45.

Device Fabrication. Highly n-type doped silicon wafers with 300 nm thermally grown SiO2 dielectric layers were purchased from Process Specialties. The gate dielectric capacitance is calculated to be 11.5 nF/cm^2 assuming a dielectric constant 3.9 of SiO_2. Wafers were cleaned by piranha solution (sulfuric acid and 30% of hydrogen peroxide 3:1 mixture (**Danger!** *Highly corrosive and oxidizing*)), deionized water, acetone, and isoproanol, followed by oxygen plasma. The cleaned substrates were treated with the vapor of hexamethyldisilazane (HMDS) or octadecyltrimethoxysilane (OTS) to make the surface hydrophobic. For the flexible transistors, ITO (120 nm, 35 ohm/sq) on PET film (0.127 mm, Aldrich) was used as substrate. This is thicker ITO than had been used in previously reported OLED bending tests.[23] A PMMA (Aldrich, M_w 120 000) layer was spin coated at 2000 rpm from chlorobenzene solution (55 mg/mL) on ITO and baked at 70 °C for 30 min. The resulting thickness was about 230 nm. The capacitance of the PMMA dielectric layer was measured to be 11.4 nF/cm^2 at 10 khz using an Agilent 4284A LCR meter. Thin films (50 nm) of organic semiconductor were deposited by vacuum evaporation (0.3−0.6 Å /s) at various substrate temperatures. Gold top contact source and drain electrodes (50 or 20 nm) were evaporated through a shadow mask.

Device Characterization. Devices were evaluated using an Agilent 4155C semiconductor analyzer in air. The channel widths were 6 mm, and lengths ranged from 250 to 275 μm measured by a ruler in the optical microscope. Mobilities were calculated from the saturation regime and fitted in the regions of highest slope.[24] X-ray diffraction scans were acquired in Bragg−Brentano ($\theta-2\theta$) geometry using a Phillips X-pert pro X-ray diffraction system. Scan parameters were: step size 0.02 ° and a time per step of 2 s. AFM images were observed by tapping mode AFM (Molecular Imaging PicoPlus).

Acknowledgment. We thank AFOSR (contract FA9550-06-1-0076), DOE (via Los Alamos National Laboratory), and the NSF MRSEC program for support of this work. We are grateful to Professor Peter Searson for access to and assistance with AFM instrumentation.

Supporting Information Available: Crystal and packing structures, AFM, electrical data, and photographs of flexible and transparent OTFTs (PDF); Crystallographic data of 1FPE-NTCDI and 2FPE-NTCDI in CIF format. This material is available free of charge via the Internet at http://pubs.acs.org.

CM802281K

(22) (a) Someya, T.; Sekitani, T.; Iba, S.; Kato, Y.; Kawaguchi, H.; Sakurai, T. *Proc. Natl. Acad. Sci., U.S.A.* **2004**, *101*, 9966. (b) Briseno, A. L.; Tseng, R. J.; Ling, M.-M.; Falcao, E. H. L.; Yang, Y.; Wudl, F.; Bao, Z. *Adv. Mater.* **2006**, *18*, 2320.

(23) Lewis, J.; Grego, S.; Chalamala, B.; Vick, E.; Temple, D. *Appl. Phys. Lett.* **2004**, *85*, 3450.

(24) Horowitz, G.; Hajlaoui, M. E.; Hajlaoui, R. *J. Appl. Phys.* **2000**, *87*, 4456.